

8. Paull, R. A. *Geology of Southeastern Wisconsin, 41st Tri-State Field Conf.* (ed. Nelson, K. G.) C-1-C-18 (1977).
9. Caputo, M. V. & Crowell, J. C., *Geol. Soc. Am. Bull.* **96**, 1020-1036 (1985).
10. Van Houten, F. B. *Paleogeogr. Paleoclimatol. Paleoecol.* **80**, 245-254 (1990).
11. Cerling, T. E. *Earth planet. Sci. Lett.* **71**, 229-240 (1984).
12. Quade, J., Cerling, T. E. & Bowman, J. R. *Geol. Soc. Am. Bull.* **101**, 464-475 (1989).
13. Reardon, E. J., Allison, G. B. & Fritz, P. *J. Hydrol.* **43**, 355-371 (1979).
14. Yapp, C. J. *Geochim. cosmochim. Acta* **55**, 2627-2634 (1991).
15. Parada, C. B., Long, A. & Davis, S. N. *Isotope Geosci.* **1**, 219-236 (1983).
16. Holser, W. *Patterns of Change in Earth Evolution* (eds Holland, H. D. & Trendall, A. F.) 123-143 (Springer, Berlin, 1984).
17. Scotese, C. R., Bambach, R. K., Barton, C., Van Der Voo, R. & Ziegler, A. M. *J. Geol.* **87**, 217-277 (1979).
18. Crowley, T. J. & North, G. R. *Paleoclimatology* (Oxford University Press, New York, 1991).
19. Van Houten, F. B. & Bhattacharyya, D. P. *Ann. Rev. Earth planet. Sci.* **10**, 441-457 (1982).
20. Van Houten, F. B. *Climate in Earth History* 112-117 (National Academy, Washington DC, 1982).

ACKNOWLEDGEMENTS. This manuscript was typed by M. Sherman. We thank B. Witzke for providing IRMWis-1, and T. Anderson for comments.

## Spatial filtering precedes motion detection

M. J. Morgan

Laboratory for Neuroscience, Department of Pharmacology, University of Edinburgh Medical School, 1 George Square, Edinburgh, Scotland, UK

WHEN we perceive motion on a television or cinema screen, there must be some process that allows us to track moving objects over time: if not, the result would be a conflicting mass of motion signals in all directions. A possible mechanism, suggested by studies of motion displacement in spatially random patterns, is that low-level motion detectors have a limited spatial range, which ensures that they tend to be stimulated over time by the same object<sup>1-3</sup>. This model predicts that the direction of displacement of random patterns cannot be detected reliably above a critical absolute displacement value ( $D_{max}$ ) that is independent of the size or density of elements in the display<sup>1,4,5</sup>. It has been inferred that  $D_{max}$  is a measure of the size of motion detectors in the visual pathway<sup>1,3</sup>. Other studies, however, have shown that  $D_{max}$  increases with element size<sup>6-8</sup>, in which case the most likely interpretation is that  $D_{max}$  depends on the probability of false matches between pattern elements following a displacement. These conflicting accounts are reconciled here by showing that  $D_{max}$  is indeed determined by the spacing between the elements in the pattern, but only after fine detail has been removed by a physiological prefiltering stage: the filter required to explain the data has a similar size to the receptive field of neurons in the primate magnocellular pathway. The model explains why  $D_{max}$  can be increased by removing high spatial frequencies from random patterns, and simplifies our view of early motion detection.

The upper motion displacement threshold ( $D_{max}$ ) was measured using random binary-luminance patterns (Fig. 1). The observers' task was to report the direction of displacement (up or down) on each trial.  $D_{max}$  was defined as the 80% correct point on the psychometric function<sup>9</sup>. The data (Fig. 2a) confirmed previous reports<sup>4,5</sup> that  $D_{max}$  is independent of element size up to about 10 arcmin. Thereafter, however,  $D_{max}$  rose sharply, reaching levels of more than 1 degree. Similar findings have been reported by Sato<sup>10</sup>. The pattern of results (a flat region followed by a linear increase) would be expected if the random patterns were spatially filtered before the displacement of edges (or other features) were detected, and if the flat region corresponded to a range of element sizes that were smaller than or similar in size to the filter<sup>7</sup>. The effect of the filter size is illustrated in Fig. 3, which shows: a random binary pattern (a); a Mexican-hat-shaped filter similar to the cross-sectional receptive field profile of retinal ganglion cells, lateral geniculate cells, and simple cortical cells<sup>11,12</sup> (b); and the convolution between the pattern and the filter (c). This is shown for three

different element sizes. The filtered profile is very similar for the two smaller element sizes but markedly different for the largest element size.

To measure the effect of different sizes of filter and pattern element, I computed the mean distance between like-signed zero-crossings in profiles such as those in Fig. 3c. The behaviour of the model is illustrated in Fig. 2b: it captures both the flat region and the region of linear increase found in the psychophysical data. The assumption in the model is that the greater

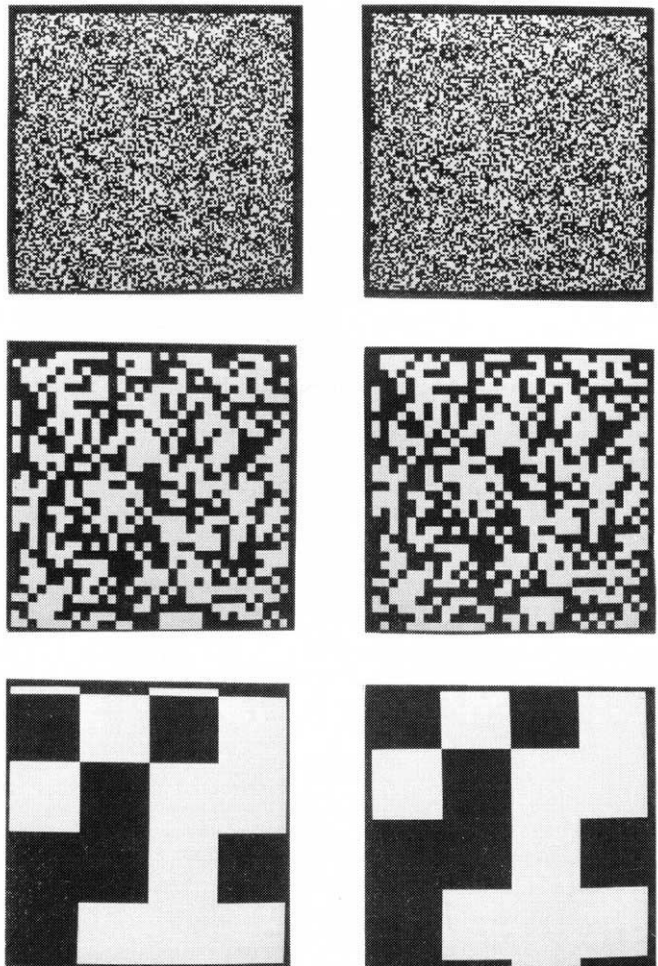


FIG. 1 Each row shows a pair of patterns that produces a perception of motion if they are presented successively in the same location. Three different element sizes are illustrated. In the experiment, the observer's task was to report the direction of motion (up or down), which was randomly varied in magnitude and direction over trials to determine  $D_{max}$ , the upper displacement limit for motion detection. To determine the threshold for each element size, eight sizes of displacement were randomly interleaved until the observer had seen ten trials of each displacement; from these data a psychometric function was constructed and the 80% correct level determined<sup>9</sup>. Each threshold was determined four times for a range of element sizes 1.2-72.0 arcmin. The observers were the author (M.M.), another experienced observer (M.F.) and two others with little previous experience of psychophysical tasks (J.H. and L.P.). In the experiment, element size was varied over a range 1-72 arcmin and  $D_{max}$  was determined for each size. The result was that  $D_{max}$  was independent of element size for sizes less than about 10 arcmin, but strongly dependent thereafter (Fig. 2). A simple filtering model (Figs 2 and 3) accounts for the data. Patterns were generated on a Mantron monochrome display at an 85 Hz frame rate, and each of the two patterns was presented for 70 ms, with a single blank frame (12 ms) interval between frames. The patterns subtended a visual angle of  $5 \times 5$  deg at the standard viewing distance by 2.28 m. The contrast of the pattern was 100% in the dark but this was reduced to 50% by ambient room lighting, which supplied a veiling luminance on the screen of about  $50 \text{ cd m}^{-2}$ .

the distance between like-signed zero-crossings, the larger the displacement that can be detected without ambiguity by matching nearest neighbour zero-crossings between the two patterns (a similar idea has been applied to stereoscopic matching<sup>13</sup>). Zero-crossings were chosen for convenience, without any implication that they are the actual primitives used in motion matching: other possibilities such as peaks, and the distance between the centroids of zero-bounded masses<sup>14</sup> gave very similar results. The separation between zero-crossings is computed only in the direction orthogonal to the motion: this simplification was justified by a subsidiary experiment with rectangular elements, which showed that elongating the elements at right angles to the direction of motion had no effect upon  $D_{\max}$ . For large element sizes the mean distance between like zero-crossings is four times the size of the pattern elements, as would be predicted from the statistics of a binary pattern independently of the filter size, and the curves intercept the  $y$ -axis when the mean distance between like-signed zero-crossings is equal to the filter space

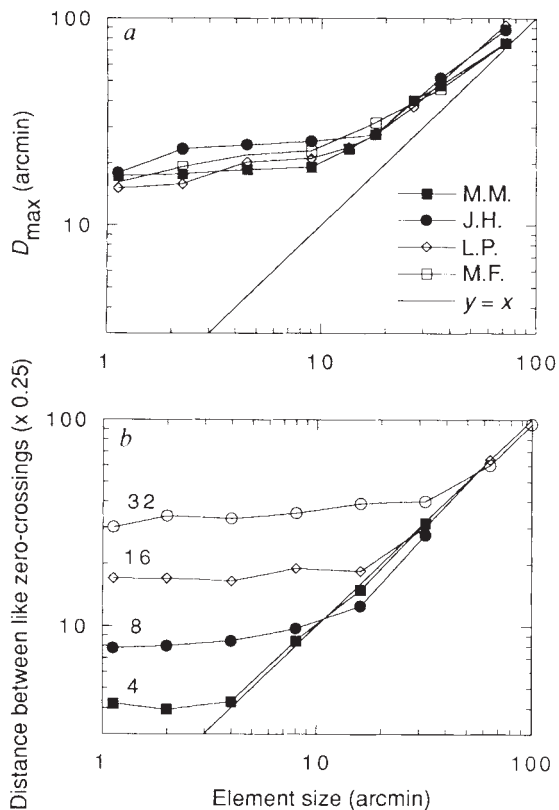


FIG. 2 Results of an experiment and a model to determine the upper limit for  $D_{\max}$  as a function of the size of elements in random patterns illustrated in Fig. 1. *a*, Results of the experiment where each set of points represents the data from a different observer. Each point is the mean of four readings.  $D_{\max}$  is nearly constant over a range 1–10 arcmin, but arises thereafter. *b*, Model to account for the shape of the curves in (*a*). Each point shows the mean of 10 independent computations based on different random stimulus profiles. Each curve shows the results for a different laplacian-of-a-gaussian filter, specified by the standard deviation of the gaussian. The diagonal straight line shows the relation  $y=x$ , where  $y$  is one quarter of the mean distance between like-signed zero-crossings. The justification for this measure is that beyond 1/4 of the distance between zero crossings, motion displacements become increasingly ambiguous. The psychophysical data also appear to converge on a unit slope between  $D_{\max}$  and element size. Note that the model curves capture the flat portion of the psychophysical curves at small element sizes. Taking into account the knee-point of the curves and their  $y$  intercept, a physiological filter with a standard deviation in the region of 8–16 arcmin would be inferred.

constant, the ideal result for filtered gaussian noise (N. Barton, personal communication).

The knee-point on the curves occurs when the standard deviation of the filter is roughly the same as the element size. Using this fact, we can estimate the standard deviation of the physiological filter to be in the region 8–16 arcmin. For the case of a laplacian-of-gaussian filter this corresponds to a receptive field centre size of 16–32 arcmin. This is probably too large to characterize foveal cells of the parvocellular pathway, but it is not incompatible with estimates of magnocellular (M) units, believed on other grounds to form the substrate of primate motion perception<sup>15</sup>. One study, for example, described few M cells in macaque monkeys as having centres smaller than 10 arcmin, with many greater than 20 arcmin<sup>16</sup>.

The convolutions illustrated in Fig. 3 were normalized in height: their amplitude diminished when the element size was smaller than the filter. This may explain the small but systematic trend in the psychophysical data towards a reduction in performance at the smallest element sizes. That this decline is not greater may well reflect the comparatively high contrast sensitivity of magnocellular neurons<sup>15,16</sup>.

The model does not claim that motion detection is limited to displacements smaller than the filter: indeed the data show orderly detection of displacements five times greater than the centre diameter. Rather, the pattern is prefiltered before the actual detection of motion occurs at a higher level, and the only limit to the matching process is in the pattern itself. The model shares with the 'elaborated Reichardt model' a localized spatial filtering preceding motion detection<sup>17</sup>, but it does not involve the additional assumption of that model that there is a fixed range of bilocal detector separations, matched to the size of the prefilter. The traditional  $D_{\max}$  value of about 15 arcmin for foveal vision reflects, not the range over which correlations can be detected, but the small sizes of element that were originally used to determine the motion threshold<sup>1</sup>, in combination with a relatively coarse prefilter.

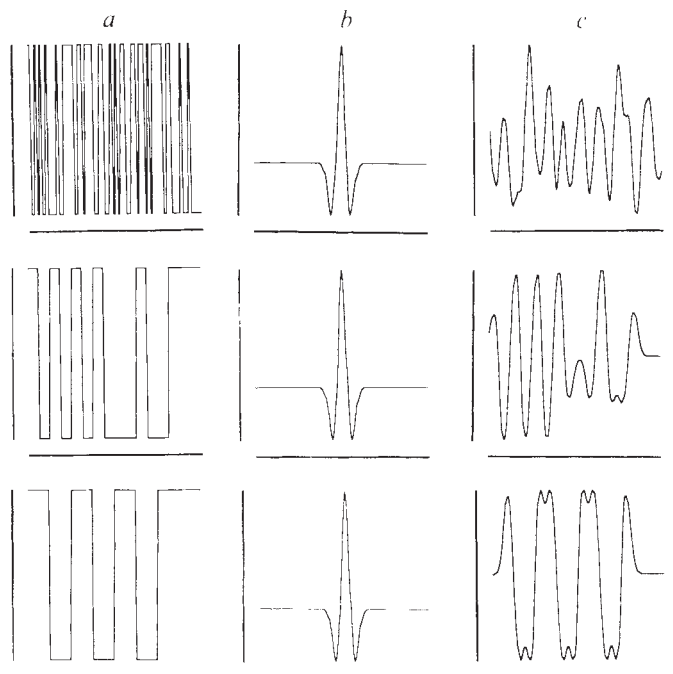


FIG. 3 *c*, Result of convolving the stimulus patterns in *a* with the filter profile in *b*. The pattern represents the luminance cross-section of a random binary pattern like those in Fig. 1. Three different element sizes are illustrated (top, middle and bottom rows). Note that the spacing between zero-crossings does not differ between the top and middle stimuli, but the spacing in the bottom row is larger.

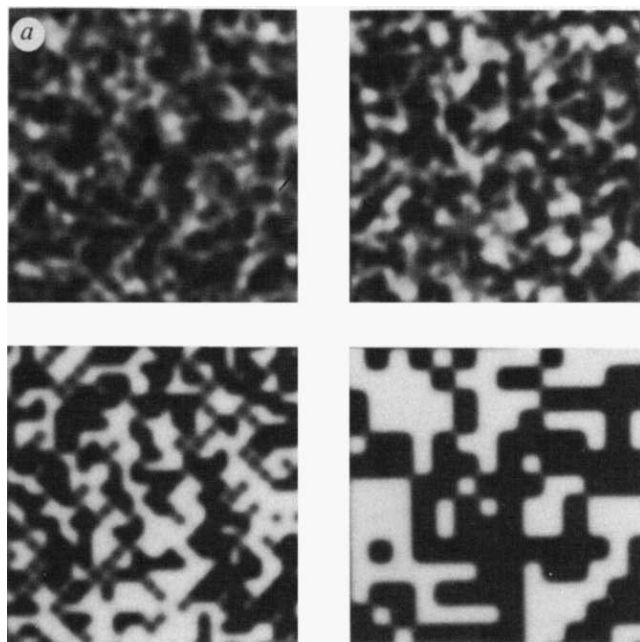
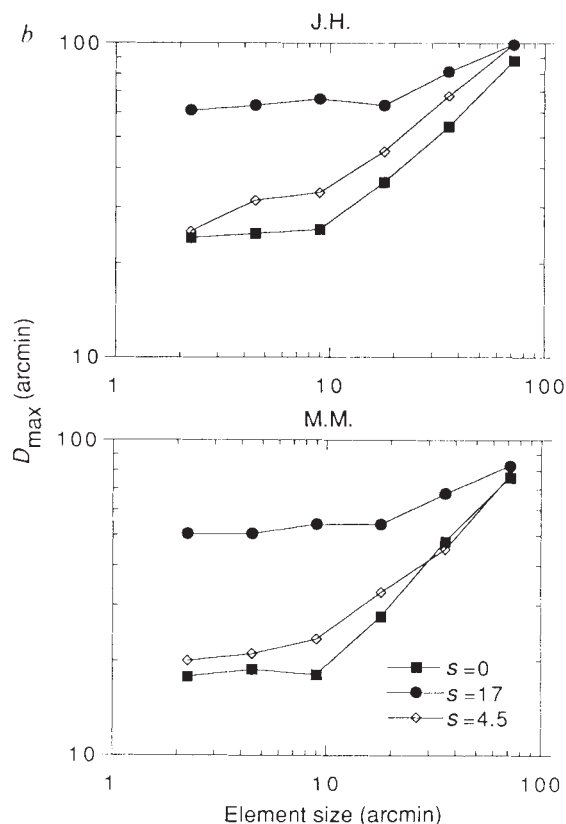


FIG. 4 *a*, Examples of low-pass filtered random binary patterns used in an experiment to measure  $D_{\max}$  as a function of original element size and filter size. The patterns were generated by convolving binary patterns with pixel size 1 (top left), 4 (top right), 8 (bottom left) and 16 (bottom right) with a gaussian filter having a standard deviation of 3.8 pixels. The original pattern had dimensions  $256 \times 256$  pixels. Note that the blob size and separation after filtering is little affected by the original pixel size, except as the largest size. This leads to the prediction that the upper motion displacement threshold  $D_{\max}$  will be little affected by element size, until the element size is large with respect to the filter: this prediction was confirmed by the

The model predicts that low-pass spatial frequency filtering (Fig. 4*a*) will extend the region over which  $D_{\max}$  is invariant with element size. If we apply a filter before the putative physiological filter, the effect should be to shift the  $D_{\max}$ /element size function to a new curve in the family in Fig. 2*b*. The experimental results in Fig. 4*b* show that this prediction is correct. The patterns were filtered by convolution with a gaussian mask, and then normalized to have the same peak-to-trough contrast as the original unfiltered patterns. A filter with a standard deviation (s.d.) of 4.5 min, which is smaller than the putative physiological filter, has little effect on the knee-point on the  $D_{\max}$ /element size curve, but a larger filter (s.d. = 17') clearly extends the flat region as well as increasing  $D_{\max}$  overall.

This analysis solves a theoretical puzzle about motion percep-



experiment result in *b*. *b*, Results of an experiment in which  $D_{\max}$  was measured as a function of element size with different amounts of prefiltering of the pattern. The data from a standard deviation of zero ( $s=0$ ) (unfiltered) are the original data from Fig. 2. For  $s=4.5$  and  $s=17$  the filters were gaussian with standard deviations of 4.5 and 17 arcmin, respectively. Results are shown for two observers (J.H. and M.M.); note that for both observers, the smaller filter has little effect on the shape of the curve, whereas the larger filter extends the region over which  $D_{\max}$  is invariant with original element size. The results may be compared with the theoretical curves in Fig. 2*a*.

tion. The displacement limit in band-limited patterns is roughly proportional to their centre spatial frequency, as would be expected from the zero-crossing model used here<sup>18,19</sup>. This has been explained by supposing that there are multiple motion filters at different spatial scales, each with its own  $D_{\max}$  value<sup>19</sup>. But the problem then is to explain why  $D_{\max}$  values for broad-band patterns, such as those used to determine  $D_{\max}$  traditionally, do not reflect the undoubted presence of low spatial frequency components in those patterns. To solve this difficulty it has been proposed<sup>19</sup> that high spatial frequency filters inhibit low spatial frequencies. The need for this elaborate scheme disappears, however, if the detection limit for both broad- and narrow-band patterns is set by the mean spatial interval between their elements, albeit after some preliminary spatial filtering. □

Received 5 August; accepted 6 November 1991.

1. Braddick, O. J. *Vision Res.* **14**, 519-527 (1974).
2. Anstis, S. M. *Phil. Trans. R. Soc.* **B290**, 153-168 (1980).
3. Braddick, O. J. *Phil. Trans. R. Soc.* **B290**, 137-151 (1980).
4. Baker, C. L. & Braddick, O. J. *Vision Res.* **22**, 1253-1260 (1982).
5. Sato, T. *Vision Res.* **29**, 1749-1758 (1989).
6. Lappin, J. S. & Bell, H. H. *Vision Res.* **16**, 161-168 (1976).
7. Cavanagh, P., Boeglén, J. & Favreau, O. *Perception* **14**, 151-162 (1985).
8. Chang, J. J. & Julesz, B. *Vision Res.* **23**, 639-646 (1983).
9. Morgan, M. J. & Cleary, R. F. *Vision Res.* (in the press).
10. Sato, T. *Perception* **19**, A7 (1990).
11. Rodieck, R. W. & Stone, J. J. *Neurophysiol.* **28**, 883-849 (1965).

12. Marr, D. & Hildreth, E. C. *Proc. R. Soc.* **B207**, 187-217 (1980).
13. Marr, D. & Poggio, T. *Proc. R. Soc.* **B204**, 301-328 (1979).
14. Watt, R. J. & Morgan, M. J. *Vision Res.* **25**, 1661-1674 (1985).
15. Schiller, P. H., Logothetis, N. K. & Charles, E. R. *Nature* **343**, 68-69 (1990).
16. Crook, J. M., Lange-Malecki, B., Lee, B. B. & Valberg, A. *J. Physiol. Lond.* **396**, 205-224 (1988).
17. Van Santen, J. P. H. & Sperling, G. *J. opt. Soc. Am.* **1**, 451-473 (1984).
18. Bischof, W. F. & DiLollo, V. *Vision Res.* **30**, 1341-1362 (1990).
19. Cleary, R. F. & Braddick, O. J. *Vision Res.* **30**, 317-327 (1990).

ACKNOWLEDGEMENTS. This work was supported by the SERC. I thank N. Barton for help in deriving the statistics of zero-crossings in random patterns and L. Partridge, G. Mather and O. Braddick for comments.